

# Interneurons accelerate learning dynamics in recurrent neural networks for statistical adaptation

David Lipshutz<sup>\*1</sup>, Cengiz Pehlevan<sup>2</sup>, and Dmitri B. Chklovskii<sup>1,3</sup>

<sup>1</sup>Center for Computational Neuroscience, Flatiron Institute

<sup>2</sup>John A. Paulson School of Engineering and Applied Sciences, Harvard University

<sup>3</sup>Neuroscience Institute, NYU Medical Center

September 23, 2022

## Abstract

Early sensory systems in the brain rapidly adapt to fluctuating input statistics, which requires recurrent communication between neurons. Mechanistically, such recurrent communication is often indirect and mediated by local interneurons. In this work, we explore the computational benefits of mediating recurrent communication via interneurons compared with direct recurrent connections. To this end, we consider two mathematically tractable recurrent neural networks that statistically whiten their inputs — one with direct recurrent connections and the other with interneurons that mediate recurrent communication. By analyzing the corresponding continuous synaptic dynamics and numerically simulating the networks, we show that the network with interneurons is more robust to initialization than the network with direct recurrent connections in the sense that the convergence time for the synaptic dynamics in the network with interneurons (resp. direct recurrent connections) scales logarithmically (resp. linearly) with the spectrum of their initialization. Our results suggest that interneurons are computationally useful for rapid adaptation to changing input statistics. Interestingly, the network with interneurons is an overparameterized solution of the whitening objective for the network with direct recurrent connections, so our results can be viewed as a recurrent neural network analogue of the implicit acceleration phenomenon observed in overparameterized feedforward linear networks.

## 1 Introduction

Efficient coding and redundancy reduction theories of neural coding hypothesize that early sensory systems decorrelate and normalize neural responses to sensory inputs [Barlow, 1961, Laughlin, 1989, Barlow and Földiák, 1989, Plumbley, 1993, Simoncelli and Olshausen, 2001, Carandini and Heeger, 2012, Westrick et al., 2016], operations that are closely related to statistical whitening of inputs. Since the input statistics are often in flux due to dynamic environments, this calls for early sensory systems that can rapidly adapt [Wark et al., 2007, Whitmire and Stanley, 2016]. Decorrelating neural activities requires recurrent communication between neurons in a population, which is typically indirect and mediated by local interneurons [Christensen et al., 1993, Shepherd

---

<sup>\*</sup>Corresponding author. E-mail: dlipshutz@flatironinstitute.org



et al., 2004]. Why do neuronal circuits for statistical adaptation mediate recurrent communication using interneurons, which take up valuable space and metabolic resources, rather than using direct recurrent connections?

A common explanation for why communication between neurons is mediated by interneurons is Dale’s principle, which states that each neuron only produces one type of neurotransmitter with exclusively inhibitory or excitatory effects on all of its targets [Strata and Harvey, 1999]. Therefore, an excitatory neuron cannot directly inhibit another neuron; rather, the inhibition must be mediated by an inhibitory interneuron. While Dale’s principle provides a physiological constraint that explains why recurrent interactions are mediated by interneurons, we seek a computational principle that can account for using interneurons rather than direct recurrent connections. This perspective is useful for a couple of reasons. First, perhaps Dale’s principle is not a hard constraint and biology could have found an efficient mechanism for a neuron to produce more than one type of neurotransmitter. In this case, a computational benefit of interneurons would provide a normative explanation for the existence of interneurons to mediate recurrent communication. Second, whitening is useful in statistical and machine learning methods [Hyvärinen and Oja, 2000, Krizhevsky, 2009, LeCun et al., 2012, Huang et al., 2018, Ermolov et al., 2021], so our analysis is potentially relevant to the design of artificial neural networks and neuromorphic systems, which are not bound by Dale’s principle. For example, interneurons are used to whiten representations in artificial neural networks for canonical correlation analysis [Golkar et al., 2020, Lipshutz et al., 2021] and independent component analysis [Pehlevan et al., 2017, Lipshutz et al., 2022].

In this work, to better understand the computational benefits of interneurons for statistical adaptation, we analyze the learning dynamics of two mathematically tractable recurrent neural networks that whiten their inputs using Hebbian/anti-Hebbian learning rules — one with direct recurrent connections and the other with indirect recurrent interactions mediated by interneurons, Figure 1. We show that the learning dynamics of the network with interneurons are more robust than the learning dynamics of the network with direct recurrent connections. In particular, we prove that the convergence time of the continuum limit of the network with direct lateral connections scales linearly with the spectrum of the initialization, whereas the convergence time of the continuum limit of the network with interneurons scales logarithmically with the spectrum of the initialization. We also numerically test the networks and, consistent with the theoretical results, find that the network with interneurons is more robust to initialization. Our results suggest that interneurons are computationally important for rapid adaptation to fluctuating input statistics.

Our analysis is closely related to analyses of learning dynamics in feedforward linear networks trained using backpropagation [Saxe et al., 2014, Arora et al., 2018, Saxe et al., 2019, Gidel et al., 2019, Tarmoun et al., 2021]. The optimization problems for deep linear networks are overparameterizations of linear problems and this overparameterization can accelerate convergence of gradient descent or gradient flow optimization — a phenomenon referred to as *implicit acceleration*. Our results can be viewed as an analogous phenomenon for the gradient flows corresponding to recurrent linear networks trained using Hebbian/anti-Hebbian learning rules. In our setting, the network with interneurons is naturally viewed as an overparameterized solution of the whitening objective for the network with direct recurrent connections. In analogy with the feedforward setting, the interneurons can be viewed as a hidden layer that overparameterizes the optimization problem.



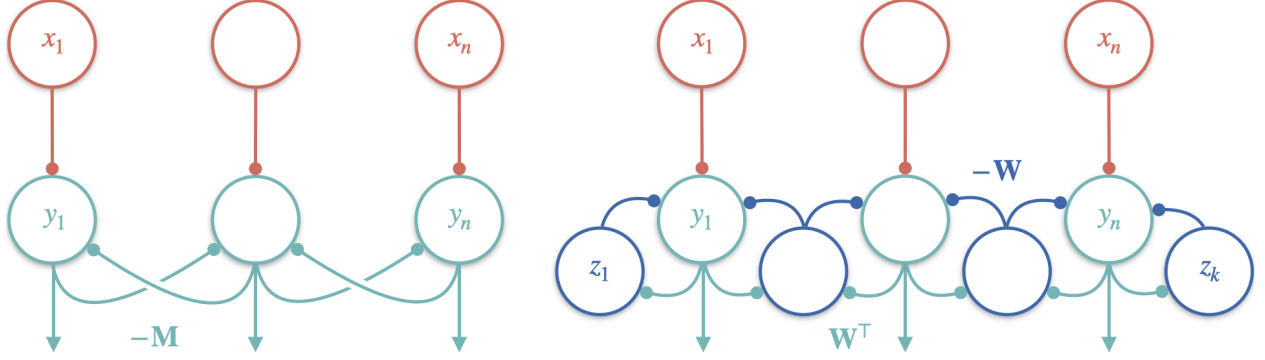


Figure 1: Recurrent networks for ZCA whitening. The network on the left has direct recurrent connections and implements Algorithm 1, whereas the network on the right has recurrent interactions mediated by interneurons (dark blue circles) and implements Algorithm 2.

## 2 Statistical whitening

Let  $\mathbf{x}_1, \dots, \mathbf{x}_T$  be a sequence of  $n$ -dimensional centered inputs, for some  $n \geq 1$ , with positive definite (empirical) covariance matrix  $\mathbf{C}_{xx} := \frac{1}{T} \mathbf{X} \mathbf{X}^\top$ , where  $\mathbf{X} := [\mathbf{x}_1, \dots, \mathbf{x}_T]$  is the  $n \times T$  data matrix of concatenated inputs. Whitening is a linear transformation of the inputs to have identity covariance matrix. In particular, an  $n \times n$  matrix  $\mathbf{F}$  is a *whitening matrix* if the outputs  $\mathbf{y}_t := \mathbf{F} \mathbf{x}_t$ , for  $t = 1, \dots, T$ , have identity covariance matrix; that is,  $\mathbf{C}_{yy} := \frac{1}{T} \mathbf{Y} \mathbf{Y}^\top = \mathbf{I}_n$ , where  $\mathbf{Y} := [\mathbf{y}_1, \dots, \mathbf{y}_T] = \mathbf{F} \mathbf{X}$  is the data matrix of concatenated outputs and  $\mathbf{I}_n$  denotes the  $n \times n$  identity matrix.

Whitening is not a unique transformation. To see this, let  $\mathbf{X} = \mathbf{U}_x (\sqrt{T} \mathbf{S}_x) \mathbf{V}_x^\top$  be the singular value decomposition of  $\mathbf{X}$ , where  $\mathbf{U}_x$  is an  $n \times n$  orthogonal matrix,  $\sqrt{T} \mathbf{S}_x = \text{diag}(\sqrt{T} \lambda_1, \dots, \sqrt{T} \lambda_n)$  is the  $n \times n$  diagonal matrix of singular values and  $\mathbf{V}_x$  is a  $T \times n$  matrix with orthonormal column vectors. Then every whitening matrix  $\mathbf{F}$  is of the form  $\mathbf{F} = \mathbf{Q} \mathbf{S}_x^{-1} \mathbf{U}_x^\top$ , where  $\mathbf{Q}$  is an arbitrary  $n \times n$  orthogonal matrix. There are several natural choices for  $\mathbf{Q}$ , each offering their own advantages [Kessy et al., 2018].

We focus on ZCA whitening [Bell and Sejnowski, 1997], also referred to as Mahalanobis whitening, which corresponds to the case  $\mathbf{Q} = \mathbf{U}_x$ , so that

$$\mathbf{F}_{\text{ZCA}} = \mathbf{U}_x \mathbf{S}_x^{-1} \mathbf{U}_x^\top = \mathbf{C}_{xx}^{-1/2}, \quad \mathbf{Y}_{\text{ZCA}} := \mathbf{F}_{\text{ZCA}} \mathbf{X} = \mathbf{U}_x \mathbf{V}_x^\top.$$

ZCA whitening minimizes the mean-square error between  $\mathbf{X}$  and  $\mathbf{Y}$  [Eldar and Oppenheim, 2003]; that is,  $\mathbf{Y}_{\text{ZCA}}$  is the unique solution to the objective

$$\arg \min_{\mathbf{Y} \in \mathbb{R}^{n \times T}} \frac{1}{T} \|\mathbf{Y} - \mathbf{X}\|_{\text{Frob}}^2 \quad \text{subject to} \quad \frac{1}{T} \mathbf{Y} \mathbf{Y}^\top = \mathbf{I}_n. \quad (1)$$

ZCA whitening is a common choice of whitening transformation used in statistical analysis and machine learning [Krizhevsky, 2009, Huang et al., 2018, Ermolov et al., 2021].

The goal of this work is a theoretical analysis of recurrent neural networks that perform ZCA whitening in the online or streaming setting using Hebbian/anti-Hebbian learning rules. The derivations of the 2 neural networks are closely related to derivations of PCA networks carried out in [Pehlevan and Chklovskii, 2015, Pehlevan et al., 2018]. For completeness, we include detailed



derivations of the neural networks here. Our main theoretical and numerical results are presented in sections 6 and 7, respectively.

### 3 Objectives for deriving ZCA whitening networks

In this section, we rewrite the ZCA whitening objective (1) to obtain 2 objectives that will be the starting points for deriving our 2 recurrent whitening networks.

#### 3.1 Objective for the network with direct recurrent connections

To derive a network with direct recurrent connections, we rewrite objective (1) to include the synaptic weight matrix of direct recurrent connections  $-\mathbf{M}$ . Expanding the square in (1), substituting in with the constraint  $\mathbf{Y}\mathbf{Y}^\top = T\mathbf{I}_n$ , dropping the terms that do not depend on  $\mathbf{Y}$  and flipping the sign yields the following objective in terms of the neural activities data matrix  $\mathbf{Y}$ :

$$\max_{\mathbf{Y} \in \mathbb{R}^{n \times T}} \frac{2}{T} \text{Tr}(\mathbf{Y}\mathbf{X}^\top) \quad \text{subject to} \quad \frac{1}{T} \mathbf{Y}\mathbf{Y}^\top = \mathbf{I}_n.$$

Next, we introduce the positive definite matrix  $\mathbf{M}$  as a Lagrange multiplier to ensure the upper bound  $\mathbf{Y}\mathbf{Y}^\top \preceq T\mathbf{I}_n$ :

$$\max_{\mathbf{Y} \in \mathbb{R}^{n \times T}} \min_{\mathbf{M} \in \mathcal{S}_{++}^n} f(\mathbf{M}, \mathbf{Y}), \quad (2)$$

where  $\mathcal{S}_{++}^n$  denotes the set of positive definite  $n \times n$  matrices and

$$f(\mathbf{M}, \mathbf{Y}) := \frac{2}{T} \text{Tr}(\mathbf{Y}\mathbf{X}^\top) - \frac{1}{T} \text{Tr}(\mathbf{M}(\mathbf{Y}\mathbf{Y}^\top - T\mathbf{I}_n)).$$

The maximization over  $\mathbf{Y}$  in objective (2) ensures that the upper bound  $\mathbf{Y}\mathbf{Y}^\top \preceq T\mathbf{I}_n$  is in fact saturated. Since  $f(\mathbf{M}, \mathbf{Y})$  is linear in  $\mathbf{M}$  and strongly concave in  $\mathbf{Y}$ , it satisfies the saddle point property (see Appendix A), so we can interchange the order of optimization. This results in the minimax objective

$$\min_{\mathbf{M} \in \mathcal{S}_{++}^n} \max_{\mathbf{Y} \in \mathbb{R}^{n \times T}} f(\mathbf{M}, \mathbf{Y}), \quad (3)$$

which is a function of neural activities and synaptic weights, and will be the starting point for our derivation of a whitening network with direct recurrent connections.

#### 3.2 Overparameterized objective for the network with interneurons

In order to derive a network with  $k \geq n$  interneurons, whose activities are encoded in the  $k \times T$  data matrix  $\mathbf{Z} = [\mathbf{z}_1, \dots, \mathbf{z}_T]$ , we replace the synaptic weight matrix  $-\mathbf{M}$  in (3) with the overparameterized matrix product  $-\mathbf{W}\mathbf{W}^\top$ , where  $\mathbf{W}$  is an  $n \times k$  full-rank matrix, which yields the minimax objective

$$\min_{\mathbf{W} \in \mathbb{R}^{n \times k}} \max_{\mathbf{Y} \in \mathbb{R}^{n \times T}} f(\mathbf{W}\mathbf{W}^\top, \mathbf{Y}).$$



The matrix  $-\mathbf{W}$  (resp.  $\mathbf{W}^\top$ ) will correspond to the synaptic weights between the interneurons (resp. principal neurons) and principal neurons (resp. interneurons). Finally, in order to arrive at an objective that also includes the interneuron activities  $\mathbf{Z}$  we substitute in with the Legendre transform:

$$-\text{Tr}(\mathbf{W}\mathbf{W}^\top\mathbf{Y}\mathbf{Y}^\top) = \min_{\mathbf{Z} \in \mathbb{R}^{k \times T}} \left\{ -2 \text{Tr}(\mathbf{Y}^\top \mathbf{W} \mathbf{Z}) + \text{Tr}(\mathbf{Z}\mathbf{Z}^\top) \right\}.$$

This results in the objective

$$\min_{\mathbf{W} \in \mathbb{R}^{n \times k}} \max_{\mathbf{Y} \in \mathbb{R}^{n \times T}} \min_{\mathbf{Z} \in \mathbb{R}^{k \times T}} g(\mathbf{W}, \mathbf{Y}, \mathbf{Z}), \quad (4)$$

where

$$g(\mathbf{W}, \mathbf{Y}, \mathbf{Z}) := \frac{2}{T} \text{Tr}(\mathbf{Y}\mathbf{X}^\top) - \frac{2}{T} \text{Tr}(\mathbf{Y}^\top \mathbf{W} \mathbf{Z}) + \frac{1}{T} \text{Tr}(\mathbf{Z}\mathbf{Z}^\top) + \text{Tr}(\mathbf{W}\mathbf{W}^\top),$$

which is a function of neural activities (including interneurons) and synaptic weights, and will be the starting point for the derivation of a whitening network with interneurons.

## 4 Derivation of a network with direct recurrent connections

Starting from the whitening objective (3), we derive an online algorithm that maps onto a network with direct recurrent connections and anti-Hebbian learning rules. The derivation of the network is closely related to the derivation of the PCA network with output whitening derived by Pehlevan et al. [2018] in the case that the feedforward matrix is fixed to be the identity matrix.

### 4.1 Offline algorithm

To derive our algorithms, we assume the recurrent neural dynamics operate at a much faster timescale than the synaptic updates. In the offline setting, at each iteration, we maximize  $f(\mathbf{M}, \mathbf{Y})$  with respect to the neural activities  $\mathbf{Y}$  and then take gradient descent steps with respect to the synaptic weight matrix  $-\mathbf{M}$ . To maximize  $f(\mathbf{M}, \mathbf{Y})$  with respect to  $\mathbf{Y}$ , we take gradient ascent steps until convergence:

$$\mathbf{Y} \leftarrow \mathbf{Y} + \gamma(\mathbf{X} - \mathbf{M}\mathbf{Y}) \quad \Rightarrow \quad \mathbf{Y} = \mathbf{M}^{-1}\mathbf{X},$$

where  $\gamma > 0$  is a small constant. After the neural activities converge, we minimize  $f(\mathbf{M}, \mathbf{Y})$  with respect to  $\mathbf{M}$  by taking a gradient descent step with respect to  $\mathbf{M}$ :

$$\mathbf{M} \leftarrow \mathbf{M} + \eta \left( \frac{1}{T} \mathbf{Y}\mathbf{Y}^\top - \mathbf{I}_n \right). \quad (5)$$

### 4.2 Online algorithm

In the online setting, at each time step  $t$ , we only have access to the input  $\mathbf{x}_t$ . In this case, we first optimize  $f(\mathbf{M}, \mathbf{Y})$  with respect to the neural activities vector  $\mathbf{y}_t$  and then take a stochastic gradient descent step with respect to the synaptic weight matrix  $\mathbf{M}$ . In particular, we first run the fast neural dynamics until convergence:

$$\mathbf{y}_t \leftarrow \mathbf{y}_t + \gamma(\mathbf{x}_t - \mathbf{M}\mathbf{y}_t) \quad \Rightarrow \quad \mathbf{y}_t = \mathbf{M}^{-1}\mathbf{x}_t.$$



After the neural activities converge, the synaptic weight matrix  $\mathbf{M}$  is updated by taking a stochastic gradient descent step:

$$\mathbf{M} \leftarrow \mathbf{M} + \eta(\mathbf{y}_t \mathbf{y}_t^\top - \mathbf{I}_n).$$

This results in Algorithm 1, which can be implemented in a network with direct recurrent connections  $-\mathbf{M}$ , Figure 1 (left). The synaptic updates are naturally interpreted as a combination of anti-Hebbian plasticity and homeostatic plasticity.

---

**Algorithm 1:** A whitening network with direct recurrent connections

---

**input** centered inputs  $\{\mathbf{x}_t\}$ ; parameters  $\gamma, \eta$   
**initialize** positive definite  $\mathbf{M}$   
**for**  $t = 1, \dots, T$  **do**  
    **repeat**  
         $\mathbf{y}_t \leftarrow \mathbf{y}_t + \gamma(\mathbf{x}_t - \mathbf{M}\mathbf{y}_t)$   
    **until** convergence  
     $\mathbf{M} \leftarrow \mathbf{M} + \eta(\mathbf{y}_t \mathbf{y}_t^\top - \mathbf{I}_n)$   
**end for**

---

## 5 Derivation of a network with interneurons

In this section, starting from the overparameterized whitening objective (4), we derive an online algorithm that maps onto a network with interneurons and Hebbian/anti-Hebbian learning rules. The derivation of the network is closely related to the derivation of the PCA network with output whitening derived by Pehlevan and Chklovskii [2015] in the case that the feedforward matrix is fixed to be the identity matrix.

### 5.1 Offline algorithm

We first optimize  $g(\mathbf{W}, \mathbf{Y}, \mathbf{Z})$  in the offline setting by alternating optimizing over the neural activities data matrices  $(\mathbf{Y}, \mathbf{Z})$  and taking a gradient descent step with respect to synaptic weight matrix  $\mathbf{W}$ . We first optimize  $g(\mathbf{W}, \mathbf{Y}, \mathbf{Z})$  with respect to the neural activities data matrices  $(\mathbf{Y}, \mathbf{Z})$  by taking gradient steps until convergence:

$$\begin{aligned} \mathbf{Y} &\leftarrow \mathbf{Y} + \gamma(\mathbf{X} - \mathbf{W}\mathbf{Z}) & \Rightarrow & \mathbf{Y} = (\mathbf{W}\mathbf{W}^\top)^{-1}\mathbf{X} \\ \mathbf{Z} &\leftarrow \mathbf{Z} + \gamma(\mathbf{W}^\top\mathbf{Y} - \mathbf{Z}) & \Rightarrow & \mathbf{Z} = \mathbf{W}^\top(\mathbf{W}\mathbf{W}^\top)^{-1}\mathbf{X}. \end{aligned}$$

After the neural activities  $(\mathbf{Y}, \mathbf{Z})$  converge, we take a gradient descent step with respect to  $\mathbf{W}$ :

$$\mathbf{W} \leftarrow \mathbf{W} + \eta \left( \frac{1}{T} \mathbf{Y}\mathbf{Z}^\top - \mathbf{W} \right). \quad (6)$$

### 5.2 Online algorithm

In the online setting, at each time step  $t$ , we first optimize  $g(\mathbf{W}, \mathbf{Y}, \mathbf{Z})$  with respect to the neural activities vectors  $(\mathbf{y}_t, \mathbf{z}_t)$  and then take a stochastic gradient descent step with respect to the



synaptic weight matrix  $\mathbf{W}$ . In particular, we first run the following gradient ascent-descent neural dynamics until convergence:

$$\begin{aligned} \mathbf{y}_t &\leftarrow \mathbf{y}_t + \gamma(\mathbf{x}_t - \mathbf{W}\mathbf{z}_t) & \Rightarrow & \mathbf{y}_t = (\mathbf{W}\mathbf{W}^\top)^{-1}\mathbf{x}_t \\ \mathbf{z}_t &\leftarrow \mathbf{z}_t + \gamma(\mathbf{W}^\top\mathbf{y}_t - \mathbf{z}_t) & \Rightarrow & \mathbf{z}_t = \mathbf{W}^\top(\mathbf{W}\mathbf{W}^\top)^{-1}\mathbf{x}_t. \end{aligned}$$

After the neural activities  $(\mathbf{y}_t, \mathbf{z}_t)$  converge, the synaptic weight matrix  $\mathbf{W}$  is updated by taking a stochastic gradient descent step:

$$\mathbf{W} \leftarrow \mathbf{W} + \eta(\mathbf{y}_t\mathbf{z}_t^\top - \mathbf{W}).$$

This results in Algorithm 2, which can be implemented in a recurrent neural network with recurrent interactions mediated by interneurons, Figure 1 (right). The synaptic updates for  $-\mathbf{W}$  (resp.  $\mathbf{W}^\top$ ) are naturally interpreted as a combination of anti-Hebbian (resp. Hebbian) plasticity and homeostatic plasticity.

---

**Algorithm 2:** A whitening network with interneurons

---

**input** centered inputs  $\{\mathbf{x}_t\}$ ; parameters  $\gamma, \eta$   
**initialize** full rank  $\mathbf{W}$   
**for**  $t = 1, \dots, T$  **do**  
  **repeat**  
     $\mathbf{y}_t \leftarrow \mathbf{y}_t + \gamma(\mathbf{x}_t - \mathbf{W}\mathbf{z}_t)$   
     $\mathbf{z}_t \leftarrow \mathbf{z}_t + \gamma(\mathbf{W}^\top\mathbf{y}_t - \mathbf{z}_t)$   
  **until** convergence  
   $\mathbf{W} \leftarrow \mathbf{W} + \eta(\mathbf{y}_t\mathbf{z}_t^\top - \mathbf{W})$   
**end for**

---

## 6 Analyses of continuous synaptic dynamics

In this section, we present our main theoretical results on convergence of the continuous synaptic dynamics for  $\mathbf{M}$  and  $\mathbf{W}$  that correspond to the updates in Algorithms 1 and 2, respectively.

### 6.1 Gradient descent algorithms

We first show that the offline updates in equations (5) and (6) are naturally viewed as gradient descent algorithms for minimizing objectives  $U(\mathbf{M})$  and  $V(\mathbf{W})$ , respectively, where

$$U(\mathbf{M}) := \max_{\mathbf{Y} \in \mathbb{R}^{n \times T}} f(\mathbf{M}, \mathbf{Y}) = \text{Tr}(\mathbf{M}^{-1}\mathbf{C}_{xx} - \mathbf{M})$$

and  $V(\mathbf{W}) = U(\mathbf{W}\mathbf{W}^\top)$  is the overparameterization of  $U(\mathbf{M})$ :

$$V(\mathbf{W}) := \max_{\mathbf{Y} \in \mathbb{R}^{n \times T}} \min_{\mathbf{Z} \in \mathbb{R}^{k \times T}} g(\mathbf{W}, \mathbf{Y}, \mathbf{Z}) = \text{Tr}\left((\mathbf{W}\mathbf{W}^\top)^{-1}\mathbf{C}_{xx} - \mathbf{W}\mathbf{W}^\top\right).$$

In particular, substituting into the offline update (5) with the optimal  $\mathbf{Y} = \mathbf{M}^{-1}\mathbf{X}$ , we see that the offline update for  $\mathbf{M}$  is

$$\mathbf{M} \leftarrow \mathbf{M} + \eta(\mathbf{M}^{-1}\mathbf{C}_{xx}\mathbf{M}^{-1} - \mathbf{I}_n) = \mathbf{M} - \eta\nabla U(\mathbf{M}).$$



Substituting into the offline update (6) with the optimal  $\mathbf{Y} = (\mathbf{W}\mathbf{W}^\top)^{-1}\mathbf{X}$  and  $\mathbf{Z} = \mathbf{W}^\top\mathbf{Y}$ , we see that the offline update for  $\mathbf{W}$  is

$$\mathbf{W} \leftarrow \mathbf{W} + \eta \left( (\mathbf{W}\mathbf{W}^\top)^{-1} \mathbf{C}_{xx} (\mathbf{W}\mathbf{W}^\top)^{-1} \mathbf{W} - \mathbf{W} \right) = \mathbf{W} - \eta \nabla V(\mathbf{W}).$$

Similarly, Algorithms 1 and 2 are naturally viewed as stochastic gradient descent methods for minimizing  $U(\mathbf{M})$  and  $V(\mathbf{W})$ , respectively.

A common approach for studying stochastic gradient descent algorithms is to analyze the corresponding continuous *gradient flows* [Saxe et al., 2014, 2019, Tarmoun et al., 2021], which are more mathematically tractable and are useful approximations of the average behavior of the stochastic gradient descent dynamics when the step size is small. In the remainder of this section, we analyze and compare the continuous gradient flows associated with Algorithms 1 and 2.

To further facilitate the analysis, we also consider so called ‘spectral initializations’  $\mathbf{M}_0$  and  $\mathbf{W}_0\mathbf{W}_0^\top$  that commute with  $\mathbf{C}_{xx}$  [Saxe et al., 2014, 2019, Gidel et al., 2019, Tarmoun et al., 2021]. Specifically, we say that  $\mathbf{A}_0 \in \mathcal{S}_{++}^n$  is a *spectral initialization* if  $\mathbf{A}_0 = \mathbf{U}_x \text{diag}(\sigma_1(0), \dots, \sigma_n(0)) \mathbf{U}_x^\top$ , where we recall that  $\mathbf{U}_x$  is the  $n \times n$  orthogonal matrix whose column vectors are the eigenvectors of  $\mathbf{C}_{xx}$  (and the left-singular vectors of  $\mathbf{X}$ ). To characterize the convergence rates of the gradient flows, we define the Lyapunov function

$$\ell(\mathbf{A}) := \|\mathbf{C}_{xx} - \mathbf{A}^2\|_{\text{Frob}}, \quad \mathbf{A} \in \mathcal{S}_{++}^n.$$

## 6.2 Gradient flow analysis of Algorithm 1

The gradient flow of  $U(\mathbf{M})$  is given by

$$\frac{d\mathbf{M}(t)}{dt} = -\nabla U(\mathbf{M}(t)) = \mathbf{M}(t)^{-1} \mathbf{C}_{xx} \mathbf{M}(t)^{-1} - \mathbf{I}_n. \quad (7)$$

Note that the offline update for  $\mathbf{M}$  is simply an Euler discretization of the gradient flow (7). To analyze solutions of  $\mathbf{M}(t)$ , we focus on spectral initializations.

**Lemma 1.** *Suppose  $\mathbf{M}_0$  is a spectral initialization. Then the solution  $\mathbf{M}(t)$  of the ODE (7) is of the form  $\mathbf{M}(t) = \mathbf{U}_x \text{diag}(\sigma_1(t), \dots, \sigma_n(t)) \mathbf{U}_x^\top$  where  $\sigma_i(t)$ ,  $i = 1, \dots, n$ , are the solutions of the ODE*

$$\frac{d\sigma_i(t)}{dt} = \frac{\lambda_i^2}{\sigma_i(t)^2} - 1, \quad i = 1, \dots, n. \quad (8)$$

Consequently,

$$\frac{d}{dt}(\sigma_i(t)^2 - \lambda_i^2)^2 = -\frac{4}{\sigma_i(t)}(\sigma_i(t)^2 - \lambda_i^2)^2, \quad i = 1, \dots, n. \quad (9)$$

*Proof.* Let  $\sigma_1(t), \dots, \sigma_n(t)$  be solutions of the ODE (8) and define  $\mathbf{M}(t) := \mathbf{U}_x \text{diag}(\sigma_1(t), \dots, \sigma_n(t)) \mathbf{U}_x^\top$ . Then

$$\frac{d\mathbf{M}(t)}{dt} = \mathbf{U}_x \text{diag} \left( \frac{\lambda_1^2}{\sigma_1(t)^2}, \dots, \frac{\lambda_n^2}{\sigma_n(t)^2} \right) \mathbf{U}_x^\top - \mathbf{I}_n = \mathbf{M}(t)^{-1} \mathbf{C}_{xx} \mathbf{M}(t)^{-1} - \mathbf{I}_n.$$

In particular, we see that  $\mathbf{M}(t)$  must be the unique solution of the ODE (7), where uniqueness of solutions follows because the right-hand-side of (7) is locally Lipschitz continuous. Equation (9) then follows from the ODE (8) and the chain rule.  $\square$



From Lemma 1, we see that for a spectral initialization with  $\sigma_i(0) \approx \lambda_i$ , the dynamics of  $\sigma_i(t)$  are approximately

$$\frac{d}{dt}(\sigma_i(t)^2 - \lambda_i^2)^2 \approx -\frac{4}{\lambda_i}(\sigma_i(t)^2 - \lambda_i^2)^2.$$

It follows that  $\sigma_i(t)^2$  converges to  $\lambda_i^2$  approximately exponentially with convergence rate  $\frac{2}{\sqrt{\lambda_i}}$ . Therefore, if  $\mathbf{M}(0)$  is a spectral initialization with  $\sigma_i(0) \approx \lambda_i$  for  $i = 1, \dots, n$ , then the convergence of  $\mathbf{M}(t)^2$  to  $\mathbf{C}_{xx}$  is approximately exponentially with convergence rate  $\frac{2}{\sqrt{\lambda_{\max}}}$ , where  $\lambda_{\max} := \max_i \lambda_i$ . A similar result, but with the inequality “ $\leq$ ” in place of the approximation “ $\approx$ ”, holds when  $\sigma_i(t) < \lambda_i$ .

On the other hand, suppose  $\sigma_i(0) \gg \lambda_i$ . From equation (8), we see that while  $\sigma_i(t) \gg \lambda_i$ ,  $\sigma_i(t)$  decays at approximately unit rate; that is,

$$\frac{d\sigma_i(t)}{dt} \approx -1. \quad (10)$$

Therefore, the time for  $\sigma_i(t)$  to converge to  $\lambda_i$  grows linearly with  $\sigma_i(0)$ . We make these statements precise in the following proposition.

**Proposition 1.** *Suppose  $\mathbf{M}_0$  is a spectral initialization and let  $\mathbf{M}(t)$  denote the solution of the ODE (7) starting from  $\mathbf{M}_0$ . If  $\sigma_i \leq \lambda_i$  for all  $i = 1, \dots, n$ , then for  $\epsilon < \ell(\mathbf{M}_0)$ ,*

$$\min\{t \geq 0 : \ell(\mathbf{M}(t)) \leq \epsilon\} \leq \frac{\sqrt{\lambda_{\max}}}{2} \log(\ell(\mathbf{M}_0)\epsilon^{-1}), \quad (11)$$

where  $\lambda_{\max} := \max_i \lambda_i$ . On the other hand, if  $\sigma_i > \lambda_i$  for some  $i = 1, \dots, n$ , then for  $\epsilon < \sigma_i^2 - \lambda_i^2$ ,

$$\min\{t \geq 0 : \ell(\mathbf{M}(t)) \leq \epsilon\} \geq \sigma_i - \sqrt{\lambda_i^2 + \epsilon}. \quad (12)$$

*Proof.* Suppose  $\sigma_i(0) \leq \lambda_i$  for  $i = 1, \dots, n$ . By equation (9),  $\sigma_i(t) \leq \lambda_i$  for all  $t \geq 0$  and so

$$(\sigma_i(t)^2 - \lambda_i^2)^2 \leq (\sigma_i(0)^2 - \lambda_i^2)^2 \exp\left(-\frac{4t}{\sqrt{\lambda_i}}\right), \quad i = 1, \dots, n.$$

Therefore,

$$\ell(\mathbf{M}(t))^2 = \sum_{i=1}^m (\sigma_i(t)^2 - \lambda_i^2)^2 \leq \ell(\mathbf{M}_0)^2 \exp\left(-\frac{4t}{\sqrt{\lambda_{\max}}}\right).$$

It follows that (11) holds. Now suppose  $\sigma_i(0) \geq \lambda_i$  for some  $i = 1, \dots, n$ . By Lemma 1,

$$\sigma_i(t)^2 - \lambda_i^2 \geq (\sigma_i(0) - t)^2 - \lambda_i^2, \quad t \in [0, \sigma_i(0) - \lambda_i].$$

It follows that (12) holds. □



### 6.3 Gradient flow analysis of Algorithm 2

The gradient flow of the overparameterized cost  $V(\mathbf{W})$  is given by

$$\frac{d\mathbf{W}(t)}{dt} = -\nabla V(\mathbf{W}) = \left(\mathbf{W}(t)\mathbf{W}(t)^\top\right)^{-1} \mathbf{C}_{xx} \left(\mathbf{W}(t)\mathbf{W}(t)^\top\right)^{-1} \mathbf{W}(t) - \mathbf{W}(t). \quad (13)$$

Given a solution  $\mathbf{W}(t)$  do the ODE (13), define  $\mathbf{A}(t) := \mathbf{W}(t)\mathbf{W}(t)^\top$ . Then

$$\frac{d\mathbf{A}(t)}{dt} = \mathbf{A}(t)^{-1} \mathbf{C}_{xx} + \mathbf{C}_{xx} \mathbf{A}(t)^{-1} - 2\mathbf{A}(t). \quad (14)$$

Note that the dynamics of  $\mathbf{A}(t)$  do not depend on  $k \geq n$ . In the following proposition, we show that  $\ell(\mathbf{A}(t))$  converges to zero exponentially for any initialization  $\mathbf{W}_0$ .

**Proposition 2.** *Let  $\mathbf{W}(t)$  denote the solution of the ODE (13) starting from any  $\mathbf{W}_0 \in \mathbb{R}^{n \times k}$ . Let  $\epsilon < \ell(\mathbf{W}_0\mathbf{W}_0^\top)$ . Suppose  $\mathbf{W}_0\mathbf{W}_0^\top$  is a spectral initialization. Then*

$$\min\{t \geq 0 : \ell(\mathbf{W}(t)\mathbf{W}(t)^\top) \leq \epsilon\} = \frac{1}{4} \log \left( \ell(\mathbf{W}_0\mathbf{W}_0^\top) \epsilon^{-1} \right). \quad (15)$$

For general initializations  $\mathbf{W}_0\mathbf{W}_0^\top$ ,

$$\min\{t \geq 0 : \ell(\mathbf{W}(t)\mathbf{W}(t)^\top) \leq \epsilon\} \leq \frac{1}{2} \log \left( \ell(\mathbf{W}_0\mathbf{W}_0^\top) \epsilon^{-1} \right). \quad (16)$$

*Proof.* By the chain rule and (14), for all  $t \geq 0$ ,

$$\begin{aligned} \frac{d\ell(\mathbf{A}(t))^2}{dt} &= 4 \operatorname{Tr} \left( (\mathbf{A}(t)^2 - \mathbf{C}_{xx}) \mathbf{A}(t) \frac{d\mathbf{A}(t)}{dt} \right) \\ &= -4 \operatorname{Tr} (\mathbf{A}(t)^2 - \mathbf{C}_{xx})^2 - 4 \operatorname{Tr} ((\mathbf{A}(t)^2 - \mathbf{C}_{xx})(\mathbf{A}(t)^2 - \mathbf{A}(t)\mathbf{C}_{xx}\mathbf{A}(t)^{-1})) \\ &= -4\ell(\mathbf{A}(t))^2 - 4\|\mathbf{A}(t)^{-1/2}(\mathbf{A}(t)^2 - \mathbf{C}_{xx})\mathbf{A}(t)^{1/2}\|_{\text{Frob}}^2. \end{aligned}$$

Suppose  $\mathbf{W}_0\mathbf{W}_0^\top$  is a spectral initialization. Then  $\mathbf{A}(t)$  commutes with  $\mathbf{C}_{xx}$  and so

$$\frac{d\ell(\mathbf{A}(t))^2}{dt} = -8\ell(\mathbf{A}(t))^2 \quad \Rightarrow \quad \ell(\mathbf{A}(t)) = \ell(\mathbf{A}(0)) \exp(-4t).$$

Thus, (15) holds. For general initializations,

$$\frac{d\ell(\mathbf{A}(t))^2}{dt} \leq -4\ell(\mathbf{A}(t))^2 \quad \Rightarrow \quad \ell(\mathbf{A}(t)) \leq \ell(\mathbf{A}(0)) \exp(-2t).$$

Therefore, inequality (16) holds.  $\square$

## 7 Numerical experiments

In this section, we numerically test the offline and online algorithms on synthetic datasets.

$$\text{Whitening error}(t) = \|\mathbf{A}_t^{-1} \mathbf{C}_{xx} \mathbf{A}_t - \mathbf{I}_n\|_{\text{Frob}},$$

and compare the evolution of the eigenvalues for  $\mathbf{A}_t = \mathbf{M}_t, \mathbf{W}_t\mathbf{W}_t^\top$ , where the subscript  $t$  indicates the value of matrices after the  $t^{\text{th}}$  iterate. To quantify the convergence time, we define

$$\text{Convergence time} := \min\{t \geq 1 : \text{Whitening error}(t) < 0.1\}.$$



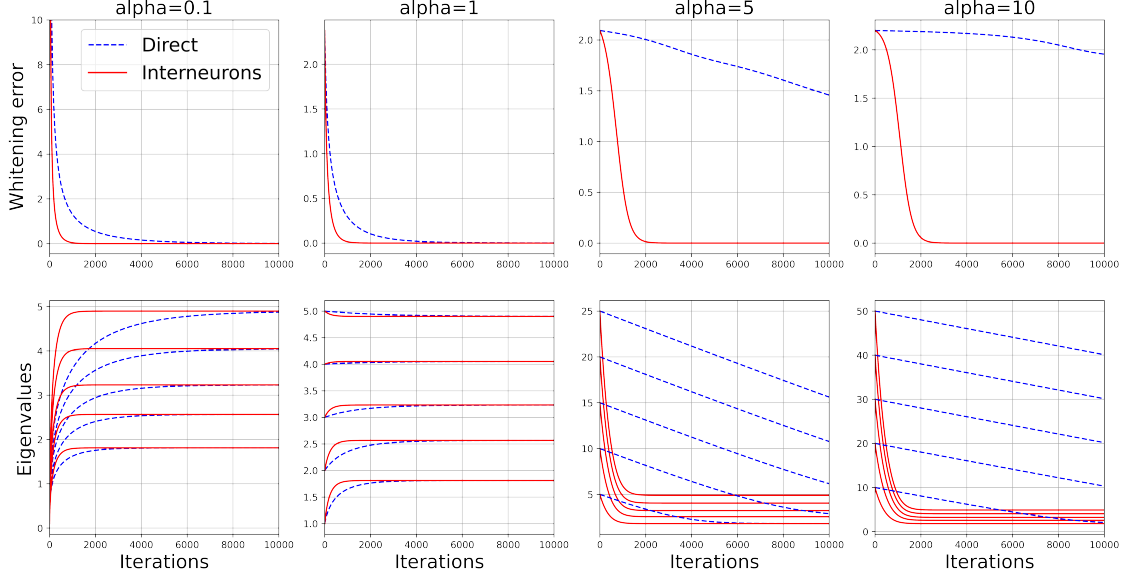


Figure 2: Comparison of whitening error and eigenvalue evolution for offline algorithms with *spectral* initializations.

### 7.1 Offline algorithms

Let  $n = 5$ ,  $k = 10$  and  $T = 10^5$ . We generate a data matrix  $\mathbf{X}$  with i.i.d. entries  $x_{t,i}$  chosen uniformly from the interval  $(0, 12)$ . The eigenvalues of  $\mathbf{C}_{xx}$  are  $\lambda_1^2 = 24.01$ ,  $\lambda_2^2 = 16.42$ ,  $\lambda_3^2 = 10.45$ ,  $\lambda_4^2 = 6.59$ ,  $\lambda_5^2 = 3.28$ . We initialize the weight matrix  $\mathbf{W}$  as follows:

$$\mathbf{W}_0 = \mathbf{Q}\sqrt{\alpha}\mathbf{\Sigma}\mathbf{P}^\top, \quad \alpha > 0, \quad \mathbf{\Sigma} := \text{diag}(5, 4, 3, 2, 1), \quad (17)$$

where  $\mathbf{Q}$  is an  $n \times n$  orthogonal matrix and  $\mathbf{P}$  is a random  $k \times n$  orthogonal matrix with orthonormal column vectors. We set  $\mathbf{M}_0 = \mathbf{W}_0\mathbf{W}_0^\top = \alpha\mathbf{Q}\mathbf{\Sigma}^2\mathbf{Q}^\top$ . We consider both spectral initializations (i.e.,  $\mathbf{Q} = \mathbf{U}_x$ ) and nonspectral initializations (i.e.,  $\mathbf{Q}$  is random orthogonal matrix). We set the step size to  $\eta = 10^{-3}$ .

**Spectral initializations.** We first consider spectral initializations (i.e.,  $\mathbf{Q} = \mathbf{U}_x$ ), which are covered by our theoretical results. The results of running the offline algorithms for  $\alpha = 0.1, 1, 5, 10$  are shown in Figure 2. Consistent with Propositions 1 and 2, the network with direct recurrent connections converges slowly for ‘large’  $\alpha$ , whereas the network with interneurons converges exponentially for all  $\alpha$ . Furthermore, as predicted by equation (10), when the eigenvalues of  $\mathbf{M}$  are ‘large’, i.e.,  $\sigma_i \gg \lambda_i$ , they decay linearly.

**Nonspectral initializations.** Next, we consider nonspectral initializations (i.e.,  $\mathbf{Q}$  is chosen uniformly at random from the set of orthogonal matrices). The results of running the offline algorithms for  $\alpha = 0.1, 1, 5, 10$  are shown in Figure 3. As with spectral initializations, the network with direct recurrent connections converges slowly large  $\alpha$  with linear decay of the spectrum for large  $\alpha$ , whereas the network with interneurons is robust to  $\alpha$ . In contrast to the case of spectral initializa-



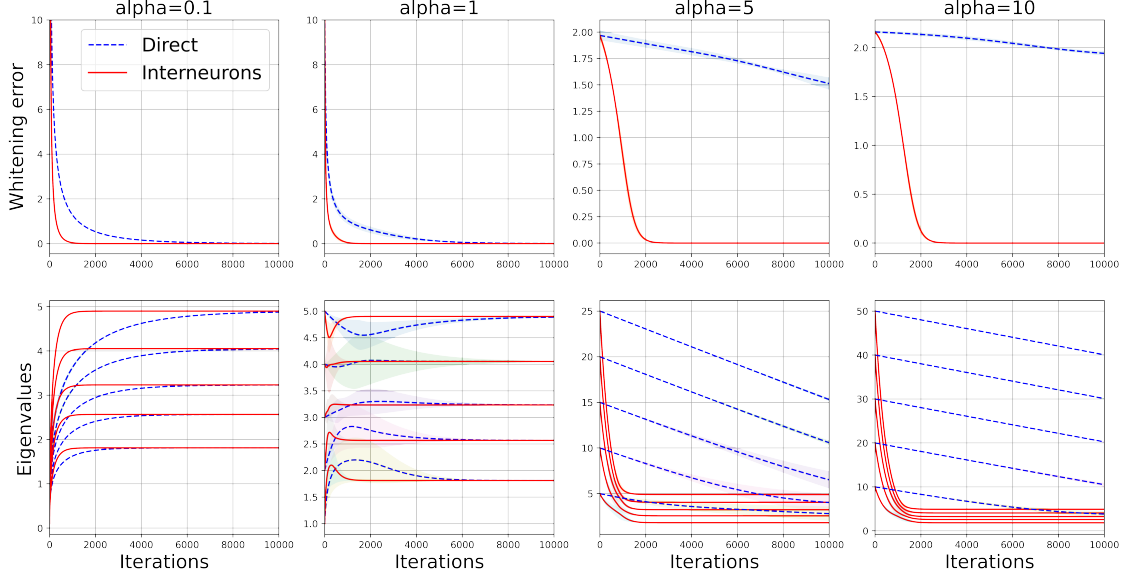


Figure 3: Comparison of whitening error and eigenvalue evolution for offline algorithms with *non-spectral* initializations. The lines and shaded regions respectively denote the means and 95% confidence intervals over 10 runs.

tions, the evolution of the eigenvalues  $\sigma_i(t)$  is not always monotone for nonspectral initializations, see the bottom row of Figure 3.

**Convergence times.** In Figure 4, we plot the convergence times of the offline algorithms with spectral and nonspectral initializations, for  $\alpha = 1, 2, \dots, 20$ . Consistent with our analysis of the gradient flows, the convergence times for network with direct lateral connections (resp. interneurons) grows linearly (resp. logarithmically) with  $\alpha$  and for large  $\alpha$  they become significantly greater than the convergence times for the network in interneurons. Interestingly, for the network with direct lateral connections, the mean convergence times for nonspectral initializations are slightly shorter ( $\sim 1.8\%$ ) than the convergence times for the spectral initializations, whereas, for the network with interneurons, the mean convergences times for nonspectral initializations are longer ( $\sim 12.4\%$ ) than the convergence times for spectral initializations .

## 7.2 Online algorithms

To test our online algorithms, we generate a synthetic dataset with samples from 2 distributions. We first set  $n = 2$ ,  $k = 4$  and fixed 2 covariance matrices

$$\mathbf{C}_A = \mathbf{U}_A \text{diag}(4, 25) \mathbf{U}_A^\top, \quad \mathbf{C}_B = \mathbf{U}_B \text{diag}(9, 16) \mathbf{U}_B^\top,$$

where  $\mathbf{U}_A, \mathbf{U}_B$  are chosen uniformly at random from the set of  $2 \times 2$  rotation matrices. We then set  $T =$  and generated a  $2 \times 4T$  dataset  $\mathbf{X} = [\mathbf{x}_1, \dots, \mathbf{x}_{4T}]$  with i.i.d. samples  $\mathbf{x}_1, \dots, \mathbf{x}_T, \mathbf{x}_{2T+1}, \dots, \mathbf{x}_{3T}$  (resp.  $\mathbf{x}_{T+1}, \dots, \mathbf{x}_{2T}, \mathbf{x}_{3T+1}, \dots, \mathbf{x}_{4T}$ ) drawn according to a mean zero Gaussian distribution with covariance matrix  $\mathbf{C}_A$  (resp.  $\mathbf{C}_B$ ). We evaluate Algorithms 1 and 2 on the dataset  $\mathbf{X}$  with constant learning rates  $\eta = 10^{-4}$  and initializations  $\mathbf{M}_0 = \mathbf{W}_0 \mathbf{W}_0^\top$ , where  $\mathbf{W}_0 = \mathbf{Q} \text{diag}(\sigma_1, \sigma_2) \mathbf{P}^\top$ ,  $\mathbf{Q}$  is a



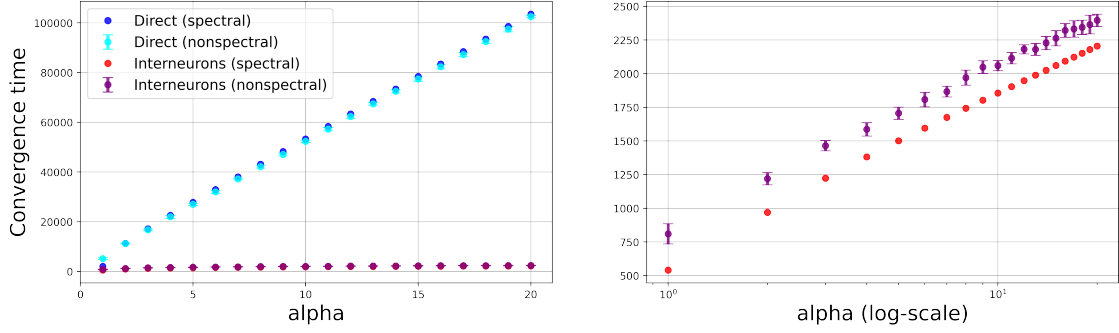


Figure 4: Comparison of convergence times for the offline algorithms with both spectral and non-spectral initializations, as functions of  $\alpha = 1, 2, \dots, 20$ . The left plot shows the convergence times for both offline algorithms. The right plot shows the convergence times for the offline algorithm corresponding the network with interneurons with  $\alpha$  plotted on a log-scale. For the nonspectral initializations, the dots and error bars respectively denote the means and 95% confidence intervals over 10 runs.

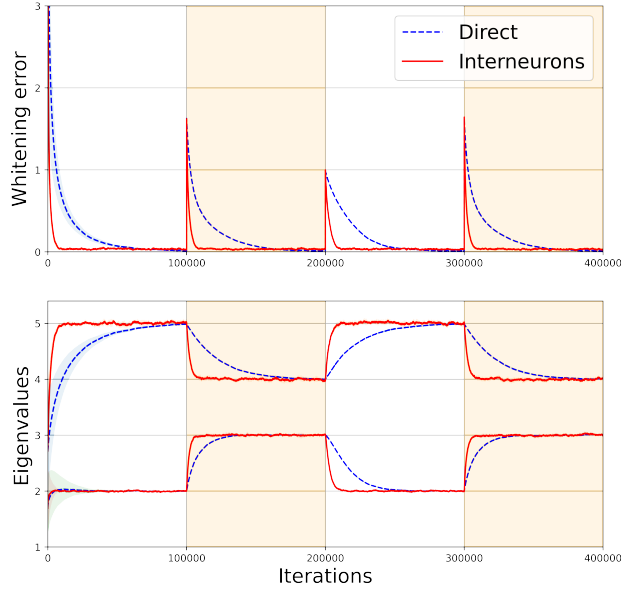


Figure 5: Comparison of whitening error and eigenvalue evolution for the online algorithms on a dataset with switching distributions. The regions with white (resp. light orange) backgrounds denote context A (resp. context B). The lines and shaded regions respectively denote the means and 95% confidence intervals over 10 runs.



random  $2 \times 2$  rotation matrix,  $\mathbf{P}$  is a random  $4 \times 2$  matrix with orthonormal column vectors and  $\sigma_1, \sigma_2$  are independent random variables chosen uniformly from the interval  $(1, 3/2)$ . The results are shown in Figure 5. Consistent with our theoretical analyses and numerical experiments in the offline setting, we see that the network with interneurons adapts to changing distributions much faster than the network with direct recurrent connections.

## 8 Conclusion

We analyzed the gradient flow dynamics of a 2 recurrent neural networks for ZCA whitening — one with direct recurrent connections and one with interneurons. For spectral initializations we can analytically estimate the convergence time for both gradient flows. For nonspectral initializations, we show that the convergence times are close to the spectral initializations with the same initial eigenvalues. Both our theoretical and numerical results show that the recurrent neural network with interneurons is more robust to initialization than the recurrent neural network with direct recurrent connections.

An interesting question is whether including interneurons in other classes of recurrent neural networks also accelerates the learning dynamics of those networks. We hypothesize that interneurons accelerate learning dynamics when the objective for the network with interneurons can be viewed as an overparameterization of the objective for the recurrent neural network with direct connections.

**Acknowledgements.** We thank Yanis Bahroun, Nikolai Chapochnikov, Lyndon Duong, Johannes Friedrich, Siavash Golkar, Jason Moore and Tiberiu Teşileanu for helpful feedback on an earlier draft of this work. C. Pehlevan acknowledges support from the Intel Corporation.

## A Saddle point property

Here we recall the following minimax property for a function that satisfies the saddle point property [Boyd and Vandenberghe, 2004, section 5.4].

**Theorem 1.** *Let  $V \subseteq \mathbb{R}^n$ ,  $W \subseteq \mathbb{R}^m$  and  $f : V \times W \rightarrow \mathbb{R}$ . Suppose  $f$  satisfies the saddle point property; that is, there exists  $(\mathbf{a}^*, \mathbf{b}^*) \in V \times W$  such that*

$$f(\mathbf{a}^*, \mathbf{b}) \leq f(\mathbf{a}^*, \mathbf{b}^*) \leq f(\mathbf{a}, \mathbf{b}^*), \quad \text{for all } (\mathbf{a}, \mathbf{b}) \in V \times W.$$

*Then*

$$\min_{\mathbf{a} \in V} \max_{\mathbf{b} \in W} f(\mathbf{a}, \mathbf{b}) = \max_{\mathbf{b} \in W} \min_{\mathbf{a} \in V} f(\mathbf{a}, \mathbf{b}) = f(\mathbf{a}^*, \mathbf{b}^*).$$

## References

Sanjeev Arora, Nadav Cohen, and Elad Hazan. On the optimization of deep networks: Implicit acceleration by overparameterization. In *International Conference on Machine Learning*, pages 244–253. PMLR, 2018.



- Horace Barlow and Peter Földiák. *Adaptation and Decorrelation in the Cortex*, page 54–72. Addison-Wesley Longman Publishing Co., Inc., USA, 1989. ISBN 020118348X.
- Horace B Barlow. Possible principles underlying the transformation of sensory messages. *Sensory Communication*, 1(01), 1961.
- Anthony J Bell and Terrence J Sejnowski. The “independent components” of natural scenes are edge filters. *Vision Research*, 37(23):3327–3338, 1997.
- Stephen Boyd and Lieven Vandenberghe. *Convex Optimization*. Cambridge University Press, 2004.
- Matteo Carandini and David J Heeger. Normalization as a canonical neural computation. *Nature Reviews Neuroscience*, 13(1):51–62, 2012.
- TA Christensen, BR Waldrop, ID Harrow, and JG Hildebrand. Local interneurons and information processing in the olfactory glomeruli of the moth *manduca sexta*. *Journal of Comparative Physiology A*, 173(4):385–399, 1993.
- Yonina C Eldar and Alan V Oppenheim. MMSE whitening and subspace whitening. *IEEE Transactions on Information Theory*, 49(7):1846–1851, 2003.
- Aleksandr Ermolov, Aliaksandr Siarohin, Enver Sangineto, and Nicu Sebe. Whitening for self-supervised representation learning. In *International Conference on Machine Learning*, pages 3015–3024. PMLR, 2021.
- Gauthier Gidel, Francis Bach, and Simon Lacoste-Julien. Implicit regularization of discrete gradient dynamics in linear neural networks. *Advances in Neural Information Processing Systems*, 32, 2019.
- Siavash Golkar, David Lipshutz, Yanis Bahroun, Anirvan Sengupta, and Dmitri Chklovskii. A simple normative network approximates local non-hebbian learning in the cortex. *Advances in Neural Information Processing Systems*, 33:7283–7295, 2020.
- Lei Huang, Dawei Yang, Bo Lang, and Jia Deng. Decorrelated batch normalization. In *Proceedings of the IEEE Conference on Computer Vision and Pattern Recognition*, pages 791–800, 2018.
- Aapo Hyvärinen and Erkki Oja. Independent component analysis: algorithms and applications. *Neural networks*, 13(4-5):411–430, 2000.
- Agnan Kessy, Alex Lewin, and Korbinian Strimmer. Optimal whitening and decorrelation. *The American Statistician*, 72(4):309–314, 2018.
- Alex Krizhevsky. Learning multiple layers of features from tiny images. Master’s thesis, University of Toronto, 2009.
- Simon B Laughlin. The role of sensory adaptation in the retina. *Journal of Experimental Biology*, 146(1):39–62, 1989.
- Yann A LeCun, Léon Bottou, Genevieve B Orr, and Klaus-Robert Müller. Efficient backprop. In *Neural networks: Tricks of the trade*, pages 9–48. Springer, 2012.



- David Lipshutz, Yanis Bahroun, Siavash Golkar, Anirvan M Sengupta, and Dmitri B Chklovskii. A biologically plausible neural network for multichannel canonical correlation analysis. *Neural Computation*, 33(9):2309–2352, 2021.
- David Lipshutz, Cengiz Pehlevan, and Dmitri B Chklovskii. Biologically plausible single-layer networks for nonnegative independent component analysis. *Biological Cybernetics*, 2022.
- Cengiz Pehlevan and Dmitri B Chklovskii. A normative theory of adaptive dimensionality reduction in neural networks. *Advances in Neural Information Processing Systems*, 28, 2015.
- Cengiz Pehlevan, Sreyas Mohan, and Dmitri B Chklovskii. Blind nonnegative source separation using biological neural networks. *Neural Computation*, 29(11):2925–2954, 2017.
- Cengiz Pehlevan, Anirvan M Sengupta, and Dmitri B Chklovskii. Why do similarity matching objectives lead to Hebbian/anti-Hebbian networks? *Neural Computation*, 30(1):84–124, 2018.
- Mark D Plumbley. A Hebbian/anti-Hebbian network which optimizes information capacity by orthonormalizing the principal subspace. In *1993 Third International Conference on Artificial Neural Networks*, pages 86–90. IET, 1993.
- Andrew M Saxe, James L McClelland, and Surya Ganguli. Exact solutions to the nonlinear dynamics of learning in deep linear neural networks. In *International Conference on Learning Representations (ICLR)*, 2014.
- Andrew M Saxe, James L McClelland, and Surya Ganguli. A mathematical theory of semantic development in deep neural networks. *Proceedings of the National Academy of Sciences*, 116(23):11537–11546, 2019.
- Gordon M Shepherd, Chen Wei R, and Charles A Greer. Olfactory bulb. In Gordon M Shepherd, editor, *The Synaptic Organization of the Brain*, chapter 5, pages 165–216. Oxford University Press, 2004.
- Eero P Simoncelli and Bruno A Olshausen. Natural image statistics and neural representation. *Annual Review of Neuroscience*, 24(1):1193–1216, 2001.
- Piergiorgio Strata and Robin Harvey. Dale’s principle. *Brain Research Bulletin*, 50(5):349–350, 1999.
- Salma Tarmoun, Guilherme Franca, Benjamin D Haeffele, and Rene Vidal. Understanding the dynamics of gradient flow in overparameterized linear models. In *International Conference on Machine Learning*, pages 10153–10161. PMLR, 2021.
- Barry Wark, Brian Nils Lundstrom, and Adrienne Fairhall. Sensory adaptation. *Current Opinion in Neurobiology*, 17(4):423–429, 2007.
- Zachary M Westrick, David J Heeger, and Michael S Landy. Pattern adaptation and normalization reweighting. *Journal of Neuroscience*, 36(38):9805–9816, 2016.
- Clarissa J Whitmire and Garrett B Stanley. Rapid sensory adaptation redux: a circuit perspective. *Neuron*, 92(2):298–315, 2016.